Journal of Controlled Release 222 (2016) 97–106

Contents lists available at ScienceDirect

Journal of Controlled Release

journal homepage: www.elsevier.com/locate/jconrel

Bioabsorbable bone plates enabled with local, sustained delivery of alendronate for bone regeneration

Woojune Hur [a,b,1], Min Park [c,1], Jae Yeon Lee [c], Myung Hun Kim [c], Seung Ho Lee [c], Chun Gwon Park [d], Se-Na Kim [c], Hye Sook Min [e], Hye Jeong Min [a,b], Jin Ho Chai [f], Sang Jeong Lee [g], Sukwha Kim [b], Tae Hyun Choi [b,*], Young Bin Choy [c,d,g,**]

[a] Biomedical Research Institute, Seoul National University Hospital, Seoul 110-744, Republic of Korea
[b] Department of Plastic and Reconstructive Surgery, Institute of Human–Environment Interface Biology, College of Medicine, Seoul National University, Seoul 110-799, Republic of Korea
[c] Interdisciplinary Program in Bioengineering, College of Engineering, Seoul National University, Seoul 152-742, Republic of Korea
[d] Institute of Medical & Biological Engineering, Medical Research Center, College of Medicine, Seoul National University, Seoul 110-799, Republic of Korea
[e] Department of Preventive Medicine, Graduate School of Public Health, Seoul National University, Seoul 152-742, Republic of Korea
[f] National Research Laboratory for Cardiovascular Stem Cell, College of Medicine, Seoul National University, Seoul 110-799, Republic of Korea
[g] Department of Biomedical Engineering, College of Medicine, Seoul National University, Seoul 110-799, Republic of Korea

ARTICLE INFO

Article history:
Received 19 January 2015
Received in revised form 27 November 2015
Accepted 8 December 2015
Available online 9 December 2015

Keywords:
Alendronate
Bioabsorbable bone plate
Bone regeneration
Drug delivery

ABSTRACT

We prepared a bone plate enabled with the local, sustained release of alendronate, which is a drug known to inhibit osteoclast-mediated bone resorption and also expedite the bone-remodeling activity of osteoblasts. For this, we coated a bone plate already in clinical use (PLT-1031, Inion, Finland) with a blend of alendronate and a biocompatible polymer, azidobenzoic acid-modified chitosan (i.e., Az-CH) photo-crosslinked by UV irradiation. As we performed the in vitro drug release study, the drug was released from the coating at an average rate of 4.03 μg/day for 63 days in a sustained manner. To examine the effect on bone regeneration, the plate was fixed on an 8 mm cranial critical size defect in living rats and the newly formed bone volume was quantitatively evaluated by micro-computed tomography (micro-CT) at scheduled times over 8 weeks. At week 8, the group implanted with the plate enabled with sustained delivery of alendronate showed a significantly higher volume of newly formed bone (52.78 ± 6.84%) than the groups implanted with the plates without drug (23.6 ± 3.81%) ($p < 0.05$). The plate enabled with alendronate delivery also exhibited good biocompatibility on H&E staining, which was comparable to the Inion plate already in clinical use. Therefore, we suggest that a bone plate enabled with local, sustained delivery of alendronate can be a promising system with the combined functionality of bone fixation and its expedited repair.

1. Introduction

Bone fixation systems made of biodegradable polymers, such as poly(lactic-co-glycolic acid) (PLGA), poly(lactic acid) (PLA) or poly(glycolic acid) (PGA), have attracted a great deal of interest as they would not need a secondary removal surgery due to biodegradability [1,2]. The major compartments of the bone fixation systems are plates and screws, where the plate is positioned and fixed on a fractured bone by screws. In this way, the undesired motion of the fractured bone can be prevented until complete healing.

However, the bone fixation systems currently in clinical use do not have the functionality to treat patients with bone loss or diseases, such as osteoporosis. It was reported that approximately 11.4% of comminuted fractures induce bone loss [3], which would impair the stability of the bone fixation systems, thereby often needing a secondary surgery [3,4]. Such complications would also include infection, which was reported to occur in approximately 13.9% patients with fractured bone [5]. The osteoporotic patients often show low bone density, which delays bone healing [6] and causes severe complications, such as microfracture, malunion or a loosening of the fixation system even with adequate fixation of fractured bone [7,8]. It has been reported that the failure of bone fixation systems occurs in 2 to 10% of fractures related to osteoporosis [8,9]. For these reasons, a strategy to facilitate bone healing is needed to properly treat fractured bone without a failure of the fixation system [10].

In this sense, alendronate can be a good candidate therapeutic agent to prevent the failure of the fixation system. Alendronate has been widely used for treatment of bone diseases, such as osteoporosis, Paget's

* Corresponding author.
** Correspondence to: Y. B. Choy, Department of Biomedical Engineering, College of Medicine, Seoul National University, Seoul 110-799, Republic of Korea.
E-mail addresses: psthchoi@snu.ac.kr (T.H. Choi), ybchoy@snu.ac.kr (Y.B. Choy).
[1] These authors contributed equally as first author to this work.

http://dx.doi.org/10.1016/j.jconrel.2015.12.007
0168-3659/

disease and inflammation-related bone loss [11–13]. The drug is a significant and potent inhibitor of bone resorption as it prevents the recruitment and differentiation of osteoclasts [13,14]. Moreover, it has been recently reported that the drug can improve the recruitment, differentiation and bone-remodeling activity of osteoblasts, thereby expediting bone repair [15–17]. Alendronate has been shown to increase bone mineral density, which is especially effective in the treatment of bone loss and osteoporosis [4,18,19].

Alendronate is often administered orally or via injection; however, when being orally administered, alendronate may induce irritation in the gastrointestinal (GI) tract, as well as abdominal pain and nausea [20]. Given these drawbacks, the local delivery of alendronate can be a promising approach to therapy. Because a bone fixation system needs to be placed locally onto a fractured bone, a combined entity of bone fixation and drug delivery should be advantageous. In addition, the sustained delivery of alendronate can benefit from the continuous inhibition of bone resorption during bone healing [21–23], which should improve bone density.

In this work, therefore, we prepared a bone fixation plate with the added functionality of the local, sustained delivery of alendronate. For this, we employed a bone plate already in clinical use (PLT-1031, Inion, Finland) and coated it with 4-azidobenzoic acid-modified chitosan (i.e., Az-CH) loaded with alendronate. Az-CH was crosslinked via UV irradiation to serve as a drug diffusion barrier for the sustained delivery of alendronate [24,25]. In addition, crosslinked Az-CH can form covalent bonds with poly(lactic acid), one of the major constituents of the Inion plate [26,27], and thus, the Az-CH based coating could be stably attached on the surface of the Inion plate. Az-CH is also proven to be biocompatible to a large extent [27,28].

We characterized the coating with Fourier transform infrared spectroscopy (FTIR), and we examined its morphology by scanning electron microscopy (SEM). We also performed the in vitro drug release study in phosphate buffered saline (PBS; pH 7.4) at 37 °C with the plate coated with both Az-CH and alendronate. For the in vivo evaluation, the plates were fixed on a craniotomy defect, 8 mm in diameter, created on the skull of living rats [29]. The degree of reconstructed bone volume was quantitatively measured using micro-computed tomography (micro-CT) at a predetermined schedule for 8 weeks following implantation. The histopathologic analyses were also carried out with the tissue including the implanted plate 8 weeks after implantation with hematoxylin and eosin (H&E) staining.

2. Materials and methods

2.1. Materials

4-azidobenzoic acid was obtained from Tokyo Chemical Industry (Tokyo, Japan). Chitosan (Mw; <200 kDa, degree of deacetylation; 75–85%), N,N,N′,N′-tetramethylethylenediamine (TEMED), 1-ethyl-3-(3-dimethylaminopropyl)-carbodiimide (EDC), alendronate sodium trihydrate, acetic acid solution, o-phthaldialdehyde (OPA), 2-mercaptoethanol (2 ME) and egg-white lysozyme were all purchased from Sigma-Aldrich (MO, USA). Phosphate buffered saline (PBS, pH 7.4) was obtained from the Seoul National University Hospital Biomedical Research Institute. Bioabsorbable bone fixation plates (PLT-1031), composed of poly(trimethylene carbonate), polylactide and polyglycolide [30], were purchased from Inion (Finland). Zolazepam and tiletamine (0.3 ml/kg; Zoletil®) were supplied from Virbac (France). Xylazine (0.1 ml/kg; Rompun®) was obtained from Bayer (Germany). Betadine was obtained from Hyundai Pharm (Korea). The absorbable sutures (Vicryl 3–0; 6–0) used for animal surgery were supplied from Ethicon (NJ, USA).

2.2. Synthesis of an azidobenzoic acid-modified chitosan (Az-CH)

Az-CH was synthesized as described in a previous study. In brief, a chitosan solution was first prepared with 200 mg chitosan dissolved in 15 ml distilled water adjusted to pH 4.75 using acetic acid solution. TEMED (116.2 mg) was dissolved in 1 ml distilled water, which was then added to the chitosan solution. To this resulting solution, a mixed solution of EDC in 1 ml distilled water and 40 mg 4-azidobenzoic acid in 1 ml dimethyl sulfoxide was then added. After adjusting the pH to 5 with 1 M HCl, the reaction was carried out at room temperature overnight. The solution was filtered via a 0.22 μm-pore filter (GSWP04700, Millipore, Bedford, MA), which was then freeze-dried for 3 days to give a dry powder of Az-CH.

2.3. Preparation of bone plate samples

We prepared the three different types of bone plate samples in this work:

(1) UP: unmodified bone plates with no treatment
(2) Az-CH_P: bone plates coated with Az-CH only
(3) AL–Az-CH_P: bone plates coated with Az-CH and alendronate

As shown in Fig. 1, we first cut a whole piece of an Inion bone plate (PLT-1031, mesh type: 14 × 14 holes) into square-shaped pieces (6 × 6 mm), each with a screw hole at the center. These pieces were each used as the UP samples without further treatment. To prepare the coated samples, i.e., Az-CH_P or AL–Az-CH_P, the coating solution was first prepared: 20 mg Az-CH or a blend of 20 mg Az-CH and 25 mg alendronate was dissolved in 1 ml of 2% v/v acetic acid solution. Then, four drops of the coating solution (3 μl per drop) were added on top of the unmodified plate around the screw hole at the center, as described in Fig. 1(A). The coated samples were each placed under UV irradiation (100 W; 365 nm, Blak-Ray, UVP, USA) for 5 min to crosslink Az-CH, which were then dried at room temperature for 24 h in a dark room (Fig. 1(B)). In this work, we coated only one side of the plate that should be faced toward the fractured bone after fixation. We also avoided the screw holes from coating, which would be under severe frictional stress during fixation. For the in vivo experiments and the mechanical property evaluation, we cut the Inion plate into a piece containing three screw holes, as depicted in Fig. S1 in the Supplementary Information. The outer two holes were used to suture and fix the plate on a bone for the in vivo experiments or employed as sites for clamping for the mechanical property evaluation. The coatings were made in the same way as described above, only around the screw hole in the middle.

2.4. Characterizations of Az-CH

To confirm the formation of Az-CH with the method employed in this work [28], we performed a spectrophotometric analysis. For this, the solutions of Az-CH, chitosan and 4-azidobenzoic acid were each prepared: 20 mg Az-CH or 20 mg chitosan was completely dissolved in 1 ml of 2% acetic acid solution, and 4-azidobenzoic acid (4 mg) was dissolved in 1 ml methanol. We obtained the UV spectra of the resulting three solutions at wavelengths from 250 nm to 400 nm (UV-1800, Shimadzu, Japan). To further confirm the formation of Az-CH, we also performed a Fourier transform infrared (FTIR) analysis. For this, Az-CH, chitosan and 4-azidobenzoic acid were each milled with potassium bromide (KBr) to produce a fine power, which was then compressed into a thin pellet.

2.5. Plate characterizations

The surface of the coating on the plate samples (i.e., AL–Az-CH_P) was examined and compared with that of the non-coated, intact surface, using a scanning electron microscope (SEM; 7501F, Jeol, Japan). Prior to imaging, the sample was placed on the SEM specimen mount and sputter coated with platinum for 5 min (208HR, Cressington Scientific, England). We also conducted FTIR analysis (JASCO 6100, Japan). To do this, each plate sample was milled with potassium bromide (KBr) to produce a fine powder and then compressed into a thin pellet for analyses. The intact Az-CH and alendronate were also analyzed for comparison.

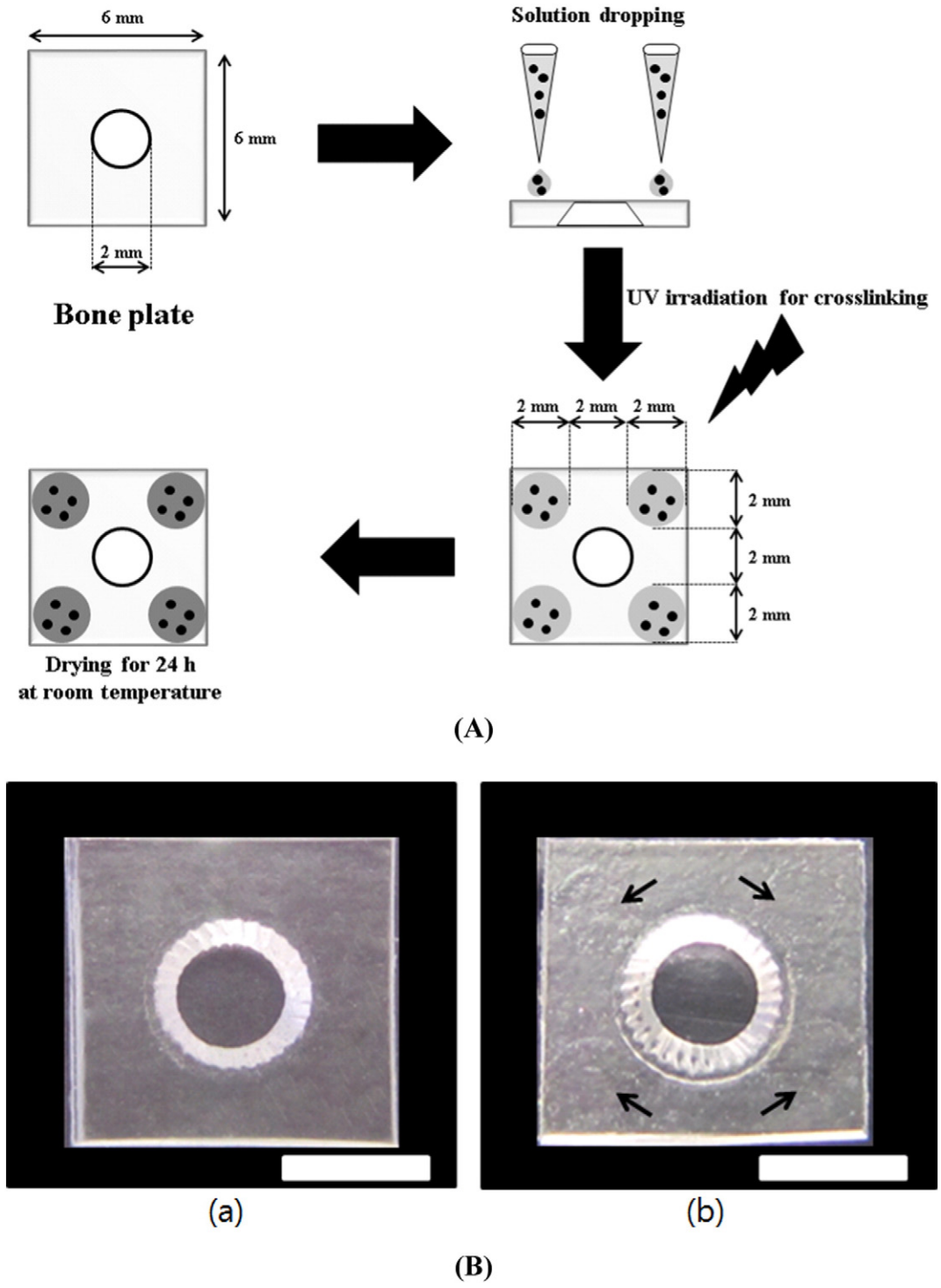

Fig. 1. (A) Schematic illustration of coating procedure. The coating solution was prepared by dissolving Az-CH or a blend of Az-CH and alendronate in an aqueous solution of acetic acid (2% v/v) for preparation of the Az-CH_P or AL–Az-CH_P, respectively. (B) Optical images of the plate samples (a) without and (b) with the coating. The arrows indicate the locations of the coatings. The scale bars represent 3 mm.

2.6. Mechanical property evaluation

To examine the mechanical properties of the plate after coating, we measured the ultimate tensile strength (UTS) of the plate samples, i.e., UP, Az-CH_P and AL–Az-CH_P (Fig. S1 in the Supplementary Information). The plate samples were each loaded in a universal testing machine (UTM; Instron-5543, MA, USA) equipped with a load cell of 71 kN, where both ends of the sample were clamped and pulled at a rate of 3 mm/min until they broke [31].

2.7. Measurement of drug-loading amount

The amount of alendronate in the coating was measured, following the method as previously employed [32]. In brief, 50 mg OPA was fully dissolved in 5 ml of an aqueous solution of 0.05 M NaOH, where 250 μl of 2 ME was added. Then, the solution was transferred to a 50 ml volumetric flask, which was then fully filled with a 0.05 M NaOH solution to give a derivatizing reagent solution (OPA/2 ME). The coating was completely scratched off from the AL–Az-CH_P, which

was then immersed in 2 ml of a lysozyme solution (4 mg/ml) at 37 °C while being agitated at 50 rpm for 72 h to fully disintegrate the Az-CH. To this 2 ml solution, a mixture of the derivatizing reagent solution (OPA/2 ME; 0.8 ml) and NaOH solution (0.05 M; 7.2 ml) was added. After 60 min, the absorbance of the resulting solution was measured spectrophotometrically (UV-1800, Shimadzu, Japan) at a wavelength of 333 nm. The experiments were performed in triplicate.

2.8. In vitro drug release study

The AL–Az-CH_P was immersed in 2 ml of phosphate buffered saline (PBS, pH 7.4) with or without lysozyme (10 μg/ml) [33] at 37 °C, which was continuously agitated at 125 rpm in a shaking incubator (SI-300, JEO TECH, Korea). At scheduled times for 77 days, the whole 2 ml release medium was collected and an equal amount of the same fresh medium was added back. The sampled media were each measured by the spectrophotometric method as described above. The experiments were performed in triplicate.

2.9. In vitro cell cytotoxicity evaluation

We used two distinct cell types (Korean Cell Line Bank, Korea), i.e., the L929 mouse fibroblasts and MG-63 cells, to assess the cytotoxicity of the plate samples prepared in this work. The L929 fibroblasts and MG-63 cells were grown in the media (WelGENE, Korea) of RPMI-1640 and DMEM, respectively, both of which were supplemented with 10% fetal bovine serum (Gibco, Life Technologies, UK) and 1% antibiotic (penicillin, 10,000 U ml^{-1}; Gibco, Life Technologies, UK). The cells were incubated in an atmosphere of 5% CO_2 in air and 100% relative humidity at 37 °C. All samples were sterilized prior to the test using ethylene oxide gas. Three batches were tested for each of the sample types.

For evaluation with L929 cells, the samples were each placed in a 24-well cell culture plate where the L929 fibroblasts were prepared at a density of 2.0×10^4 cells/well. After incubation in a humidified atmosphere with 5% CO_2 at 37 °C for 24 h (HERAcell 150i, Thermo Scientific, USA), the samples were each washed with distilled water to fully remove the non-adhered cells. Afterward, the adhered cells on the coating were quantitatively investigated. For evaluation with MG-63 cells, the plate samples were each immersed in 2 ml of the PBS medium (pH 7.4) at 37 °C for 23 days, where the sample medium was fully extracted and refreshed every 2–4 days. Among the extracted sample media, the ones at days 1, 3, 7, 13 and 23 were used for evaluation. Thus, MG-63 cells were seeded in a 96-well cell culture plate at a density of 2.0×10^4 cells/well. After 24 h incubation, the cell growth medium was fully extracted and replaced with the same amount of a mixture of fresh cell growth medium and extracted sample one (1:1; v/v). After another 24 h incubation, the cells in the well were quantitatively investigated.

For quantitative evaluation of the cells, the EZ-Cytox Cell viability assay kit was used, following the manufacturer's instruction (No. EZ-1000, DAEILAB SERVICE, Korea) [34]. The absorbance was measured at 450 nm using a microplate reader (VERSA max, Molecular Devices, USA).

2.10. In vivo animal study

For the in vivo evaluation of the plate samples, we used 8-week-old male SD rats weighing 250–300 g (Koatech, Keung-Ki, Pyong-Taek, Korea). The rats were cared and housed, following the protocol approved by the Institutional Animal Care and Use Committee (IACUC No. 13–0100) at Seoul National University Hospital. The rats were provided with food and water ad libitum. All samples were sterilized prior to implantation using ethylene oxide gas. Three batches were tested for each of the sample types.

To examine the bone regeneration effect, we first created the calvarial bone defect in rats as previously reported [35]. Anesthesia was induced by intramuscular injection of a cocktail of zolazepam and tiletamine (0.3 ml/kg; Zoletil®, Virbac, France), and xylazine (0.1 ml/kg; Rompun®, Bayer, Germany). Then, the hair on the head was clearly shaved, followed by cleaning with Betadine® (Hyundai Pharm, Korea) and the calvarial bone was exposed through a skin incision, 5 cm in length. A calvarial bone defect, 8 mm in diameter, was created with a trephine (TPHB-B8, Osung, Korea). To fix the plate in place, two holes for suturing, 10 mm apart, were also made by drilling, each of which was located 2 mm away from the boundary of a defect. The surgical area was washed with saline to fully remove bone debris. The plate sample was placed on the calvarial bone defect with the coated side facing toward the defect. Then, the plate was fixed with bioabsorbable suture (Vicryl 3–0, Ethicon, NJ, USA) through the outer

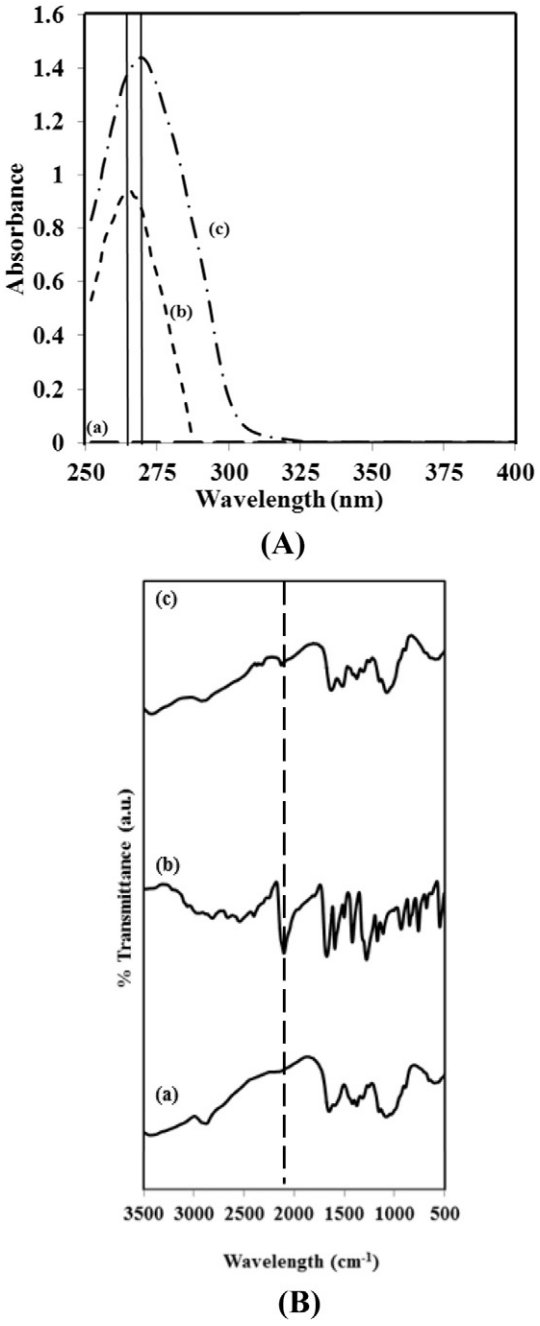

Fig. 2. (A) UV spectra of (a) chitosan, (b) 4-azidobenzoic acid, and (c) Az-CH. (B) FTIR spectra of (a) chitosan, (b) 4-azidobenzoic acid and (c) Az-CH.

two holes made for suturing (Fig. S1 in the Supplementary Information). Then, the incised skin was closed with a bioabsorbable suture and a post-operative dressing was applied with Betadine®.

According to the types of the implanted samples, the animals were divided into four groups.

(1) The no treatment group: the animals without the plate
(2) The UP group: the animals implanted with the UP
(3) The Az-CH_P group: the animals implanted with the Az-CH_P
(4) The AL–Az-CH_P group: the animals implanted with the AL–Az-CH_P

Six animals were employed for each of the implant groups and two animals (i.e., one in the UP group and the other one in the Az-CH_P group) died during the experiment. The causes of death were undeterminable and thus, those animals were excluded for data analysis. Therefore, at least five animals were tested for each of the implant groups.

To evaluate new bone formation, images from the bone defect were obtained via micro-computed tomography (micro-CT; NFR Polaris-G90, In-vivo Micro-CT, NanoFocusRay, Korea) at 1, 4 and 8 weeks after plate implantation. Imaging was performed on the scanner at an isotropic voxel size of 9 μm with an X-ray tube current of 180 μA and a voltage at 55 kV. At each time for imaging, the animal was sedated with an intramuscular injection of Zoletil® (0.3 mg/ml). From each of the micro-CT images, the regions of interest were defined, based on a cylindrical shape of the cranial defect made herein, where the new bone formation was determined by setting the gray threshold level at 200. The new bone volume percent was calculated by dividing the volume of newly formed bone by that of the initially created defect, using the AMIRA software (Version 5.4, ZIB & Visage Imaging, Germany).

2.11. Histologic and histomorphometric evaluation

Eight weeks after plate implantation, three animals per group were sacrificed with carbon dioxide and the specimens including the bone defect and plate sample were biopsied. The specimen was fixed in 10% (v/v) buffered neutral formalin for 3 days, which was then embedded with resin, sectioned into 30–40 μm-thick slides (BS-3000 N, EXAKT, Germany) and stained with hematoxylin and eosin (H&E). The slides were examined under an optical microscope (BX53F, OLYMPUS, Japan) with ×40 and ×100 magnifications for histologic evaluation by a professional pathologist. The images of the slides were also assessed for histomorphometric evaluation using Image J software (National Institute of Health, Bethesda, USA). The new bone area percent was obtained by dividing the area of newly formed bone by that of initially created defect.

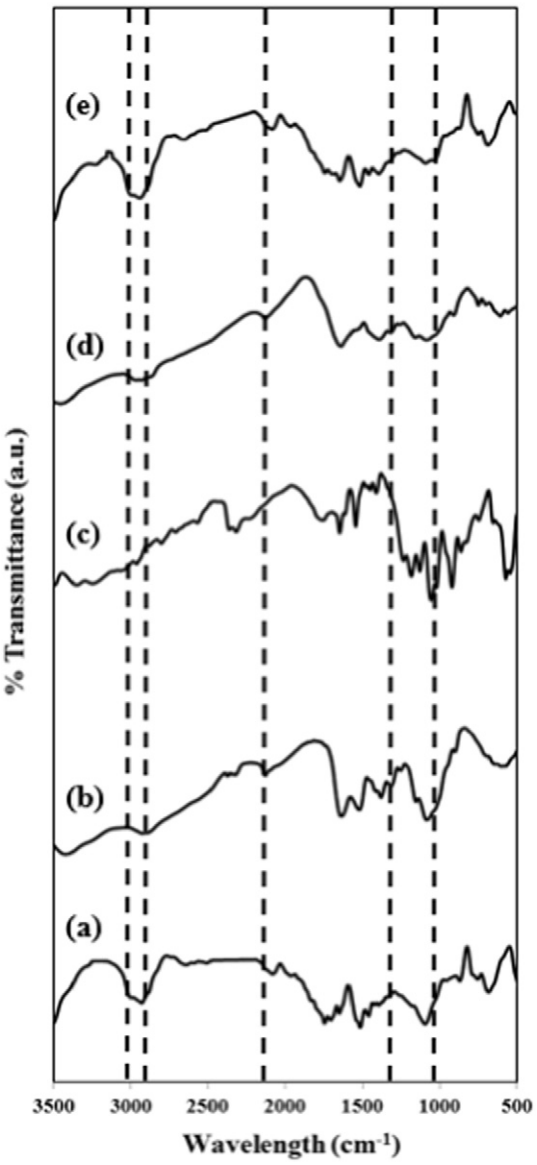

Fig. 4. FTIR spectra of (a) UP, (b) Az-CH, (c) alendronate, (d) Az-CH_P and (e) AL–Az-CH_P. The dashed lines indicate the major peaks from UP, Az-CH and alendronate, respectively.

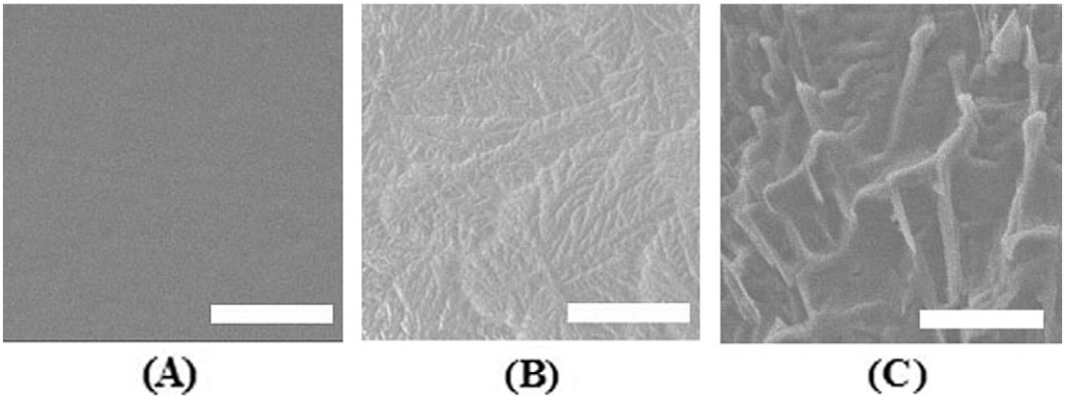

Fig. 3. Scanning electron micrographs of the surfaces (A) without and (B, C) with the coating on the AL–Az-CH_P. The scale bars represent (A, B) 100 μm and (C) 10 μm.

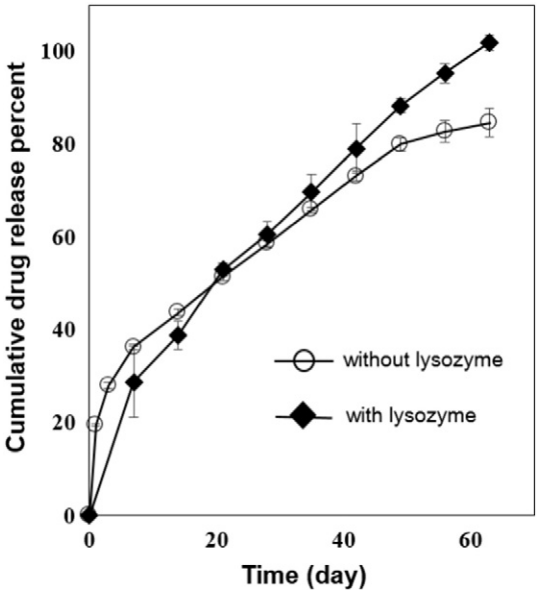

Fig. 5. In vitro drug release profiles of the AL–Az-CH_P with and without lysozyme.

2.12. Statistics

Mean percentages of new bone volumes and areas among the four different animal groups were statistically analyzed with one-way ANOVA with $\alpha = 0.05$ followed by pairwise comparisons using a Tukey's post hoc test (GraphPad Prism, version 5.01, USA). $p < 0.05$ was considered statistically significant.

3. Results

3.1. Characterization of Az-CH

To confirm the formation of Az-CH, we assessed the UV spectra of Az-CH, chitosan and 4-azidobenzoic acid, as shown in Fig. 2(A). For 4-azidobenzoic acid, an apparent peak at 266 nm was ascribed to the N_3 group. This peak was also observed for Az-CH with a shift to 272 nm, although the chitosan did not show any characteristic peaks in the spectrum [26]. This indicated that the reaction between a free amino group of the chitosan and a carboxyl group of 4-azidobenzoic acid indeed occurred to introduce the N_3 group to the chitosan [27]. To further confirm this, we also assessed the FTIR spectra. As shown in Fig. 2(B), a characteristic peak at 2127 cm^{-1} was observed with 4-azidobenzoic acid due to the N_3 group. This peak was not seen with chitosan but appeared with Az-CH, indicating again the introduction of the N_3 group to the chitosan, giving Az-CH. The degree of substitution of azidobenzoic acid in Az-CH was 1%, according to our previous study [36].

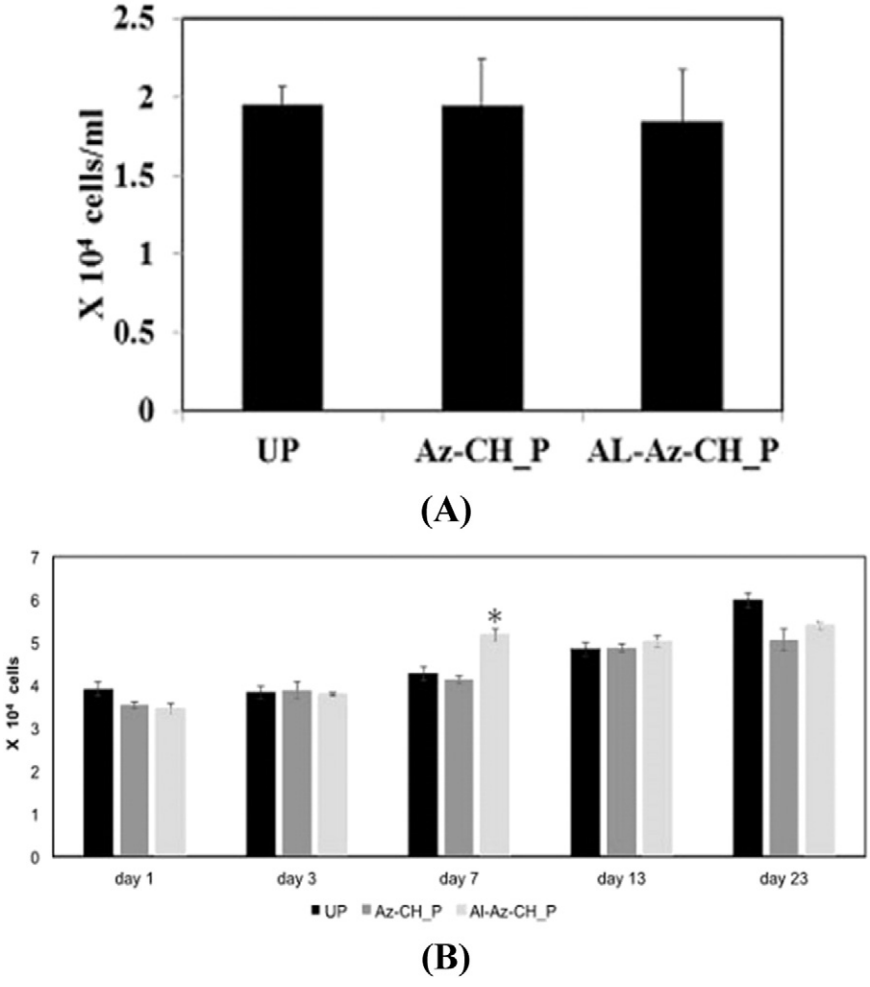

Fig. 6. Cytotoxicity evaluation of the plate samples of the UP, Az-CH_P and AL–Az-CH_P, using (A) L929 fibroblasts and (B) MG-63 cells.

3.2. Characterization of plate samples

Fig. 3 showed the scanning electron micrographs of the non-coated and coated surfaces of the AL–Az-CH_P. The non-coated, unmodified surface was observed to be smooth with almost no micro-cracks or -defects (Fig. 3(A)). On the other hand, a rough, wrinkled surface was observed on the coated surface (Fig. 3(B, C)), which appeared to be created while the coating solution was dried to leave the dry Az-CH. The surface morphology was not very different regardless of the presence of alendronate.

The amount of chitosan in each coated plate was calculated to be about 0.18 mg and the coating thickness in dry condition was measured to be 20–40 μm (Fig. S2 in the Supplementary Information). The coating appeared to be stable in PBS, showing almost no apparent sign of degradation until 120 days when visually observed (Fig. S3 in the Supplementary Information). In contrary, with the presence of the enzyme (i.e., lysozyme) [37,38], the coating was observed to gradually disappear (Fig. S3 in the Supplementary Information), implying that the coating should degrade when implanted in vivo. Meanwhile, the Inion plate employed in this work is known to fully degrade in two years [39].

We also evaluated the FTIR spectra of the plate samples to investigate the presence of either alendronate or Az-CH in the coating, as shown in Fig. 4. For the UP, the double bands near 2960 cm^{-1} and 3000 cm^{-1} were ascribed to the C–H stretching in methane group [40]. For Az-CH, the characteristic peaks were seen at wavelengths of 1320 cm^{-1} and 2127 cm^{-1}, which were due to the C–O–N and N_3 group [27,41], respectively. For alendronate, the characteristic peak at 1022 cm^{-1} was due to an asymmetric vibration of the P–OH group [42]. On the FTIR spectrum of the coated plate sample, i.e., the Az-CH_P or AL–Az-CH_P, the characteristic peaks from each of the constituents, i.e., the UP and Az-CH, or the UP, Az-CH and alendronate, respectively, were observed to be overlapped, implying the presence of all constituents. The participation of alendronate in the reaction during UV exposure is not highly expected as the drug does not possess any light absorbing groups, such as chromophores [32]. The bone plate needs to be strong enough to fix a fractured bone until healing [43]. This inherent mechanical property of the bone plate herein did not vary even after coating with the method employed in this work (Table S1 and Fig. S5 in the Supplementary Information).

3.3. In vitro drug release profile

For the AL–Az-CH_P, the loading amount of alendronate was measured to be 293.84 ± 8.04 μg per plate (i.e., 73.46 ± 2.01 μg per coating). Considering a theoretical drug-loading amount of 300 μg, the AL–Az-CH_P exhibited a high drug loading efficiency of more than 97%. This was somewhat expected as the coating herein was prepared simply by drying the drops of the drug and chitosan solution on a plate without any other treatment. Because of that, the drug was evenly distributed in the coating (Fig. S4 in the Supplementary Information). According to the in vitro drug release study, the drug was released in a sustained manner for 63 days for both media with and without lysozyme (Fig. 5). Without lysozyme, drug release was relatively fast during the first seven days with an approximate rate of 5.3% per day (i.e., 15.56 μg per day), which slowed down to the rate of 0.9% per day (i.e., 2.6 μg per day) for the rest 56 days. With lysozyme, drug release became faster than the one without lysozyme after 28 days and almost 100% drug was released in 63 days. This long-term release could be ascribed to the electrostatic and hydrogen-bonding interactions between chitosan and alendronate [22,44].

3.4. Cytotoxicity

To evaluate the cytotoxicity of the coatings, we first quantitatively analyzed the number of L929 fibroblast cells adhering to the surface of the plate samples, as shown in Fig. 6(A). The amount of adhered cells was not significantly different among the plate samples of the UP, Az-CH_P and AL–Az-CH_P. We also performed a quantitative analysis on MG-63 cells with the medium immersed with the plate samples for a long-term period of 23 days. As shown in Fig. 6(B), during the whole tested period, the number of MG-63 cells was not very different among the plate samples of the UP, Az-CH_P and AL–Az-CH_P: only at day 7, there was a noticeable increase in cell number with the AL–Az-CH_P compared with the other two samples [45]. Considering that the UP, an Inion bone plate in clinical use, is already proven to be safe to a large extent, those results suggested that the coatings prepared in this work are also not cytotoxic.

3.5. In vivo new bone formation

To examine the efficacy of the alendronate-release coating, we investigated the degree of in vivo new bone formation within the calvarial

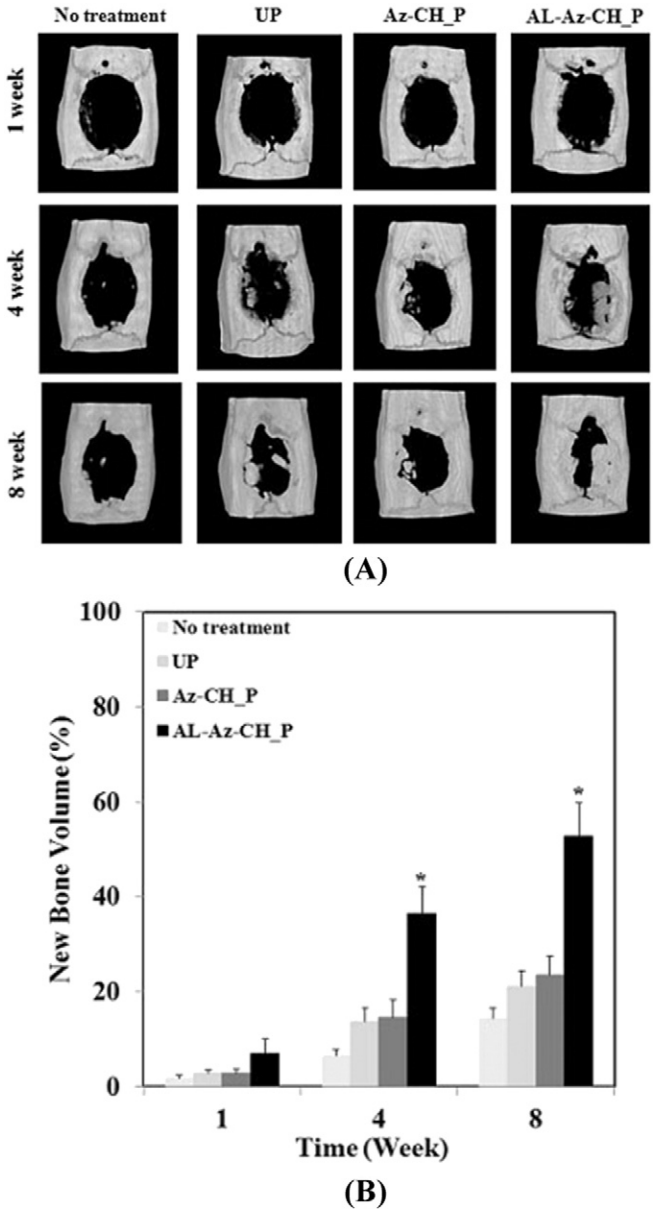

Fig. 7. Micro-CT image analysis on new bone formation in cranial defects of the animal groups with no treatment and the ones fixed with the UP, Az-CH_P and AL–Az-CH_P at 1, 4 and 8 weeks after implantation. (A) Micro-CT images and (B) new bone volume percent around the cranial defects. *At 4 and 8 weeks, the AL–Az-CH_P group was statistically significantly different from the no treatment group ($p < 0.05$).

bone defect, using micro-CT (Fig. 7). For all animal groups, the average percent of new bone volume increased as the time elapsed. However, the degree of new bone formation was slow in the animal groups without alendronate (i.e., the no treatment, UP, Az-CH_P groups), where the new bone volume percent increased to at most 14–24% at 8 weeks and at all scheduled times of imaging, their values were not statistically significantly different. In contrast, the increase in new bone was evident with the AL–Az-CH_P group. At 4 weeks, the new bone volume percent was 36.39 ± 5.58%, which increased further to 52.78 ± 6.84% at 8 weeks. Notably, the average percent of new bone volume was statistically significantly higher with the AL–Az-CH_P group from 4 weeks than those with the other different animal groups ($p < 0.05$).

3.6. Histologic and histomorphometric evaluation

The tissue of the calvarial defect was microscopically evaluated on H&E staining 8 weeks after implantation, as shown in Fig. 8 (also see Fig. S6 in the Supplementary Information). In the no treatment group, only a few bone fragments were observed, mainly at the edge of the calvarial bone defect, which seemed to be newly formed after surgery. In the UP and Az-CH_P groups, fibrous tissue surrounded the plate sample, whereas newly formed bone tissue was scarce around the plate, as seen in Fig. 8(f) and (g). In contrast, in the AL–Az-CH_P group, the newly formed bone appeared to cover most of the surface of the plate and extended to the edges of the calvarial bone defect.

At 8 weeks after surgery, for all groups, neutrophils, lymphocytes and other active inflammatory components were not observed around the plate and within the bone defect, where some amount of fibrous tissue was seen instead. Notably, the amount of fibrous tissue formation was grossly similar with all groups, i.e., the UP, Az-CH_P, and AL–Az-CH_P groups, which were approximately 10–50 μm in thickness from the plate. These findings suggested that the extent of inflammatory reaction of the Az-CH_P and AL–Az-CH_P was not significantly different from that of the UP, i.e., the Inion plate already in clinical use. To modulate such inflammation, a combined use of the formulation releasing antioxidants or anti-inflammatory drugs could be beneficial [46,47]. For example, the formulation in forms of microparticles could be easily embedded upon the coating during crosslinking in this study.

We also performed the histomorphometric analysis to quantitatively assess new bone formation. As shown in Fig. 9, the new bone area percent increased significantly with the AL–Az-CH_P, compared with the other different groups. This result was consistent with the one from the micro-CT image analysis (Fig. 7).

4. Discussion

In this work, we suggested a bone plate enabled with a therapeutic ability is potentially advantageous for the treatment of bone loss associated with comminuted fractures as well as osteoporosis. For this, we prepared a proof-of-principle device, i.e., a bone plate coated with Az-CH loaded with a drug, alendronate. Alendronate is known to stimulate

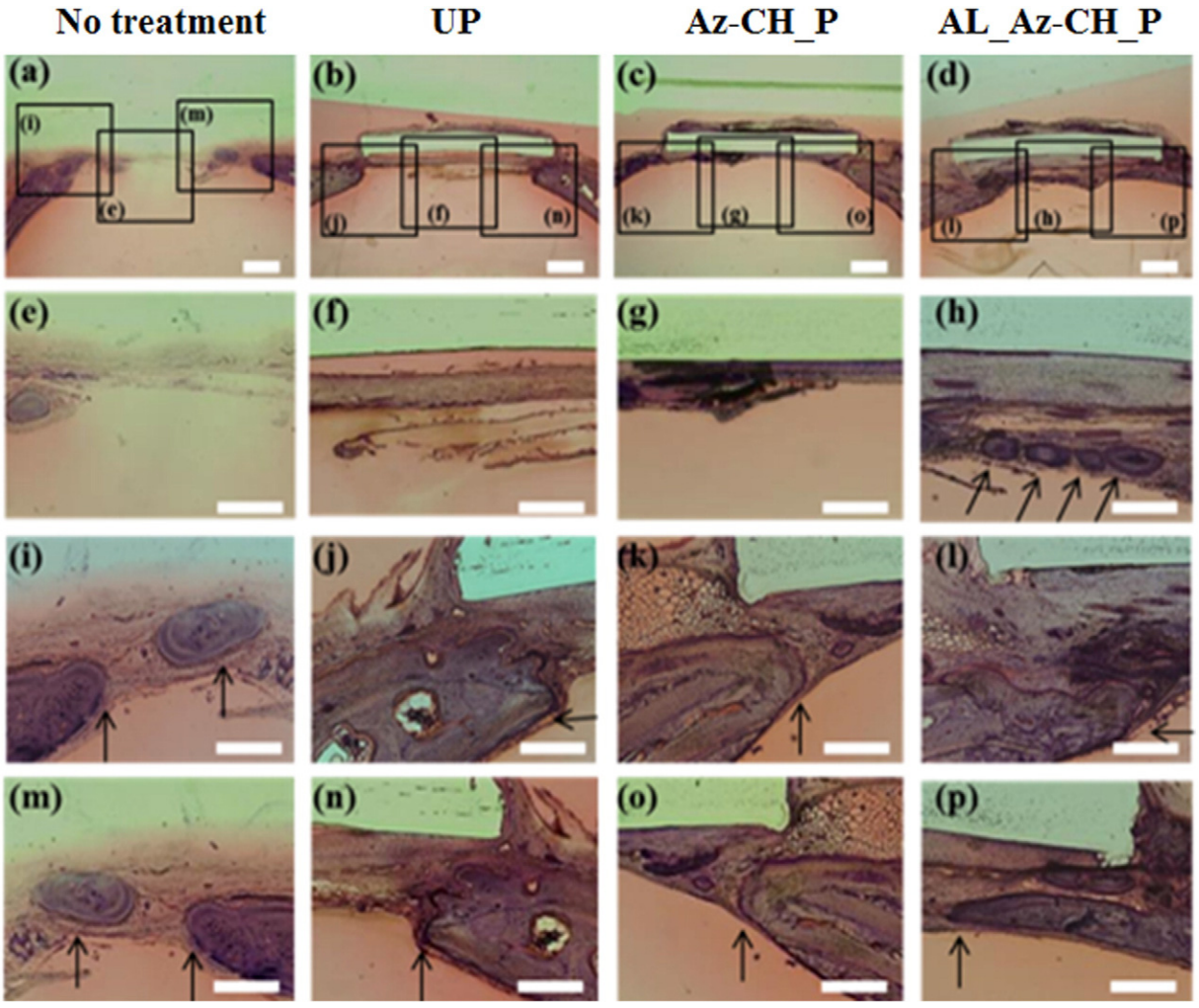

Fig. 8. Histological images from the tissue around the cranial defect obtained at 8 weeks after implantation of the plate samples. The arrows indicate the specific locations of new bone formation. The scale bars represent 100 μm.

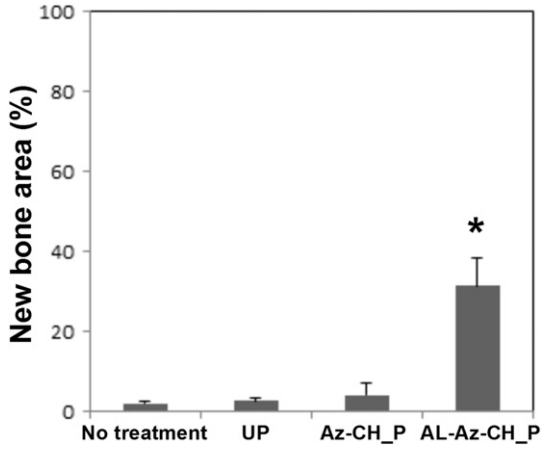

Fig. 9. Histomorphometric analysis on new bone formation in cranial defects of the animal groups with no treatment and the ones fixed with the UP, Az-CH_P and AL–Az-CH_P at 8 weeks after implantation. *The AL–Az-CH_P group was statistically significantly different from the other different groups.

the recruitment and differentiation of osteoblasts as well as inhibit bone resorption, thereby facilitating new bone formation [11,16]. For this reason, the local, sustained delivery of alendronate could be a promising way to expedite bone reconstruction.

In this work, the AL–Az-CH_P showed sustained drug release from the coating for 63 days at an average rate of approximately 4.0 μg per day (Fig. 5), which should be therapeutically effective in bone regeneration and also safe to a large extent, as many previous studies reported [48–50]. This long-term release of alendronate appeared to allow suppression of the osteoclastic activity, significant mainly at the late stage of bone healing [29,51]. As a result, for the bone defect animal models herein, the AL–Az-CH_P showed the enhanced in vivo new bone formation from 4 weeks, compared with the plate samples without alendronate (Fig. 7 and Fig. 8). However, further study is needed to fully support the final clinical advantages of the AL–Az-CH_P for treatment of fractures or bone loss with osteoporotic patients.

In this work, we employed a modified form of chitosan, Az-CH, as coating material. For the chitosan-based materials, to properly serve as drug diffusion barrier, chemical crosslinking is often incorporated, using an agent such as glutaraldehyde, epichlorohydrin, glyoxal, etc. [52–54] However, this process requires a comparably long reaction time in an aqueous environment, which may degenerate the mechanical properties of the bone plate, originally needed for bone fixation. Unlike this, the Az-CH could form a crosslinked network via UV irradiation in a short period of time (5 min) to achieve the prolonged delivery of alendronate [25,52,55]. Thus, the plate did not need to be exposed to an aqueous environment for a long time. Because of this, the plates herein appeared to retain their mechanical properties even after coating (Table S1 and Fig. S5 in the Supplementary Information). Most importantly, the Az-CH has been generally considered to be not cytotoxic [26,28], which could be also supported by the results in this work (Fig. 6).

Alendronate is usually prescribed for oral administration [56]; however, it has been reported that a long-term use of alendronate could induce adverse gastrointestinal side effects and thus, there are recommended dose limitations [57]. Previously, the proposed systems for the local delivery of alendronate were in form of scaffolds [22], grafts [58] and particles [23,59] and were evaluated to be effective to a large extent. However, for the treatment of bone fracture, those systems may require an additional procedure to apply them to the defected bone before or after implanting the bone fixation system during surgery. In this sense, a combined entity of the bone plate and drug delivery coating suggested in this work could be considered practically advantageous.

5. Conclusion

In this work, we suggest a bone plate enabled with therapeutic functionality of expedited bone regeneration. To realize this, a bone plate already in clinical use was coated with photo-crosslinked Az-CH loaded with a drug, alendronate. In this work, the drug could be released from the coating for approximately 63 days in a sustained manner, maintaining a therapeutically effective drug level. Therefore, when this alendronate-delivery plate was fixed on a calvarial critical size defect in vivo, a statistically significantly higher volume of newly formed bone was observed than those with the plates without the drug. The alendronate-delivery plate also exhibited good in vivo biocompatibility, similar to the Inion plate already in clinical use. Therefore, we conclude that a bone plate enabled with the sustained, local delivery of alendronate can be a promising system for both bone fixation and its expedited repair.

Acknowledgment

The study was supported by a grant from the KRIBB (KGM4891511) and Ministry of Health & Welfare (HI14C2310), Republic of Korea. This research was also supported by a grant of the Korea Health Technology R&D Project through the Korea Health Industry Development Institute (KHIDI), funded by the Ministry of Health & Welfare, Republic of Korea (grant number: HI14C2194) and "Advanced medical new material (fiber) development program" through the Ministry of Trade, Industry and Energy (MOTIE) and Korea Institute for Advancement of Technology (KIAT) (R00001408).

Appendix A. Supplementary data

Supplementary data to this article can be found online at http://dx.doi.org/10.1016/j.jconrel.2015.12.007.

References

[1] C.G. Ambrose, T.O. Clanton, Bioabsorbable implants: review of clinical experience in orthopedic surgery, Ann. Biomed. Eng. 32 (2004) 171–177.
[2] P.B. Maurus, C.C. Kaeding, Bioabsorbable implant material review, Oper. Techn. Sport. Med 12 (2004) 158–160.
[3] J.F. Keating, A.H.R.W. Simpson, C.M. Robinson, The management of fractures with bone loss, J. Bone Joint Surg. (Br.) 87b (2005) 142–150.
[4] R.B. Gustilo, J.T. Anderson, Prevention of infection in the treatment of one thousand and twenty-five open fractures of long bones: retrospective and prospective analyses, J. Bone Joint Surg. Am. 58 (1976) 453–458.
[5] R.H. Quinn, D.J. Macias, The management of open fractures, Wilderness Environ. Med. 17 (2006) 41–48.
[6] J.P. Rodriguez, S. Garat, H. Gajardo, A.M. Pino, G. Seitz, Abnormal osteogenesis in osteoporotic patients is reflected by altered mesenchymal stem cells dynamics, J. Cell. Biochem. 75 (1999) 414–423.
[7] J.G. Liu, X.X. Xu, Stress shielding and fracture healing, Zhonghua Yi Xue Za Zhi 74 (1994) 483–485 519.
[8] P.V. Giannoudis, E. Schneider, Principles of fixation of osteoporotic fractures, J. Bone Joint Surg. (Br.) 88B (2006) 1272–1278.
[9] M. Stover, Distal femoral fractures: current treatment, results and problems, Injury 32 (2001) 3–13.
[10] K. Stromsoe, Fracture fixation problems in osteoporosis, Injury 35 (2004) 107–113.
[11] E. Orwoll, M. Ettinger, S. Weiss, P. Miller, D. Kendler, J. Graham, S. Adami, K. Weber, R. Lorenc, P. Pietschmann, K. Vandormael, A. Lombardi, J.D. Adachi, N. Bell, J.J. Body, A. Castro, A. Daifotis, D. Felsenberg, N. Gilchrist, A. Hoffman, M. Maricic, R. Rizzoli, S. Silverman, J. Valeriano, Alendronate for the treatment of osteoporosis in men, N. Engl. J. Med. 343 (2000) 604–610.
[12] M.T. Drake, B.L. Clarke, S. Khosla, Bisphosphonates: mechanism of action and role in clinical practice, Mayo Clin. Proc. 83 (2008) 1032–1045.
[13] G.A. Rodan, H.A. Fleisch, Bisphosphonates: mechanisms of action, J. Clin. Invest. 97 (1996) 2692–2696.
[14] H.J. Moon, Y.P. Yun, C.W. Han, M.S. Kim, S.E. Kim, M.S. Bae, G.T. Kim, Y.S. Choi, E.H. Hwang, J.W. Lee, J.M. Lee, C.H. Lee, D.S. Kim, I.K. Kwon, Effect of heparin and alendronate coating on titanium surfaces on inhibition of osteoclast and enhancement of osteoblast function, Biochem. Biophys. Res. Commun. 413 (2011) 194–200.
[15] G.I. Im, S.A. Qureshi, J. Kenney, H.E. Rubash, A.S. Shanbhag, Osteoblast proliferation and maturation by bisphosphonates, Biomaterials 25 (2004) 4105–4115.
[16] C. Garcia-Moreno, S. Serrano, M. Nacher, M. Farre, A. Diez, M.L. Marinoso, J. Carbonell, L. Mellibovsky, X. Nogues, J. Ballester, J. Aubia, Effect of alendronate on cultured normal human osteoblasts, Bone 22 (1998) 233–239.

[17] G.G. Reinholz, B. Getz, L. Pederson, E.S. Sanders, M. Subramaniam, J.N. Ingle, T.C. Spelsberg, Bisphosphonates directly regulate cell proliferation, differentiation, and gene expression in human osteoblasts, Cancer Res. 60 (2000) 6001–6007.
[18] J.D. Adachi, K.G. Saag, P.D. Delmas, U.A. Liberman, R.D. Emkey, E. Seeman, N.E. Lane, J.M. Kaufman, P.E. Poubelle, F. Hawkins, Two-year effects of alendronate on bone mineral density and vertebral fracture in patients receiving glucocorticoids: a randomized, double-blind, placebo-controlled extension trial, Arthritis Rheum. 44 (2001) 202–211.
[19] H.G. Bone, D. Hosking, J.P. Devogelaer, J.R. Tucci, R.D. Emkey, R.P. Tonino, J.A. Rodriguez-Portales, R.W. Downs, J. Gupta, A.C. Santora, U.A. Liberman, I.I.I.O.T.S.G. alendronate phase, ten years' experience with alendronate for osteoporosis in postmenopausal women, N. Engl. J. Med. 350 (2004) 1189–1199.
[20] S. Aki, N. Eskiyurt, U. Akarirmak, F. Tuzun, M. Eryavuz, S. Alper, O. Arpacioglu, F. Atalay, V. Kavuncu, S. Kokino, O. Kuru, K. Nas, O. Ozerbil, G. Savas, O.F. Sendur, D. Soy, G. Akyuz, T.O. Soc, Gastrointestinal side effect profile due to the use of alendronate in the treatment of osteoporosis, Yonsei Med. J. 44 (2003) 961–967.
[21] J.D. Zhao, H. Tang, J.C. Gu, B. Wang, L. Bao, B.Q. Wang, Evaluation of a novel osteoporotic drug delivery system in vitro: alendronate-loaded calcium phosphate cement, Orthopedics 33 (2010) 546–561.
[22] S.E. Kim, D.H. Suh, Y.P. Yun, J.Y. Lee, K. Park, J.Y. Chung, D.W. Lee, Local delivery of alendronate eluting chitosan scaffold can effectively increase osteoblast functions and inhibit osteoclast differentiation, J. Mater. Sci. - Mater. Med. 23 (2012) 2739–2749.
[23] X.T. Shi, Y.J. Wang, L. Ren, Y.H. Gong, D.A. Wang, Enhancing alendronate release from a novel PLGA/hydroxyapatite microspheric system for bone repairing applications, Pharm. Res-Dord 26 (2009) 422–430.
[24] N. Bhattarai, J. Gunn, M.Q. Zhang, Chitosan-based hydrogels for controlled, localized drug delivery, Adv. Drug Deliv. Rev. 62 (2010) 83–99.
[25] K. Obara, M. Ishihara, Y. Ozeki, T. Ishizuka, T. Hayashi, S. Nakamura, Y. Saito, H. Yura, T. Matsui, H. Hattori, B. Takase, M. Ishihara, M. Kikuchi, T. Maehara, Controlled release of paclitaxel from photocrosslinked chitosan hydrogels and its subsequent effect on subcutaneous tumor growth in mice, J. Control. Release 110 (2005) 79–89.
[26] A.P. Zhu, M. Zhang, J. Wu, J. Shen, Covalent immobilization of chitosan/heparin complex with a photosensitive hetero-bifunctional crosslinking reagent on PLA surface, Biomaterials 23 (2002) 4657–4665.
[27] S. Aiba, N. Minoura, K. Taguchi, Y. Fujiwara, Covalent immobilization of chitosan derivatives onto polymeric film surfaces with the use of a photosensitive hetero-bifunctional cross-linking reagent, Biomaterials 8 (1987) 481–488.
[28] Y. Yeo, J.A. Burdick, C.B. Highley, R. Marini, R. Langer, D.S. Kohane, Peritoneal application of chitosan and UV-cross-linkable chitosan, J. Biomed. Mater. Res. A 78 (2006) 668–675.
[29] M.P. Lutolf, F.E. Weber, H.G. Schmoekel, J.C. Schense, T. Kohler, R. Müller, J.A. Hubbell, Repair of bone defects using synthetic mimetics of collagenous extracellular matrices, Nat. Biotechnol. 21 (2003) 513–518.
[30] Inion Inc., Inion CPS® Fixation System, inhttp://www.inion.com/Products/CMF_surgery/en_GB/Inion_CPS_Fixation_System/, Aug. 9th, 2015.
[31] G.J. Buijs, E.B. van der Houwen, B. Stegenga, R.R. Bos, G.J. Verkerke, Mechanical strength and stiffness of biodegradable and titanium osteofixation systems, J. Oral Maxillofac. Surg. 65 (2007) 2148–2158.
[32] S.K. Al Deeb, I.I. Hamdan, S.M. Al Najjar, Spectroscopic and HPLC methods for the determination of alendronate in tablets and urine, Talanta 64 (2004) 695–702.
[33] Y. Huang, S. Onyeri, M. Siewe, A. Moshfeghian, S.V. Madihally, In vitro characterization of chitosan-gelatin scaffolds for tissue engineering, Biomaterials 26 (2005) 7616–7627.
[34] Z. Huang, H. Lee, E. Lee, S.K. Kang, J.M. Nam, M. Lee, Responsive nematic gels from the self-assembly of aqueous nanofibres, Nat. Commun. 2 (2011) 459.
[35] P.P. Spicer, J.D. Kretlow, S. Young, J.A. Jansen, F.K. Kasper, A.G. Mikos, Evaluation of bone regeneration using the rat critical size calvarial defect, Nat. Protoc. 7 (2012) 1918–1929.
[36] C.G. Park, C. Shasteen, Z. Amoozgar, J. Park, S.-N. Kim, J.E. Lee, M.J. Lee, Y. Suh, H.K. Seok, Y. Yeo, Photo-crosslinkable chitosan hydrogel as a bioadhesive for esophageal stents, Macromol. Res. 23 (2015) 1–6.
[37] J. Hankiewi, E. Swiercze, Lysozyme in human body-fluids, Clin. Chim. Acta 57 (1974) 205–209.
[38] Y. Huang, S. Onyeri, M. Siewe, A. Moshfeghian, S.V. Madihally, In vitro characterization of chitosan–gelatin scaffolds for tissue engineering, Biomaterials 26 (2005) 7616–7627.
[39] T. Nieminen, I. Rantala, I. Hiidenheimo, J. Keranen, H. Kainulainen, E. Wuolijoki, I. Kallela, Degradative and mechanical properties of a novel resorbable plating system during a 3-year follow-up in vivo and in vitro, J. Mater. Sci. Mater. Med. 19 (2008) 1155–1163.
[40] Y. Ma, Y. Zheng, K. Liu, G. Tian, Y. Tian, L. Xu, F. Yan, L. Huang, L. Mei, Nanoparticles of poly(lactide-co-glycolide)-da-tocopheryl polyethylene glycol 1000 succinate random copolymer for cancer treatment, Nanoscale Res. Lett. 5 (2010) 1161–1169.
[41] L.L. Fernandes, C.X. Resende, D.S. Tavares, G.A. Soares, L.O. Castro, J.M. Granjeiro, Cytocompatibility of chitosan and collagen-chitosan scaffolds for tissue engineering, Polímeros 21 (2011) 1–6.
[42] C.Y. Wang, X.F. Xiao, D. Mao, H.Z. Tang, R.F. Liu, The study of using TiO2 nanotube arrays as a drug delivery for alendronate, Adv. Mater. Res. 335-336 (2011) 1469–1472.
[43] A.U. Daniels, M.K. Chang, K.P. Andriano, Mechanical properties of biodegradable polymers and composites proposed for internal fixation of bone, J. Appl. Biomater. 1 (1990) 57–78.
[44] C. Chatelet, O. Damour, A. Domard, Influence of the degree of acetylation on some biological properties of chitosan films, Biomaterials 22 (2001) 261–268.
[45] Y. Xiong, H. Yang, J. Feng, Z. Shi, L. Wu, Effects of alendronate on the proliferation and osteogenic differentiation of MG-63 cells, J. Int. Med. Res. 37 (2009) 407–416.
[46] S.D. Patil, F. Papadmitrakopoulos, D.J. Burgess, Concurrent delivery of dexamethasone and VEGF for localized inflammation control and angiogenesis, J. Control. Release 117 (2007) 68–79.
[47] T. Hickey, D. Kreutzer, D.J. Burgess, F. Moussy, In vivo evaluation of a dexamethasone/PLGA microsphere system designed to suppress the inflammatory tissue response to implantable medical devices, J. Biomed. Mater. Res. 61 (2002) 180–187.
[48] C.Z. Wang, S.M. Chen, C.H. Chen, C.K. Wang, G.J. Wang, J.K. Chang, M.L. Ho, The effect of the local delivery of alendronate on human adipose-derived stem cell-based bone regeneration, Biomaterials 31 (2010) 8674–8683.
[49] S.J. Meraw, C.M. Reeve, P.C. Wollan, Use of alendronate in peri-implant defect regeneration, J. Periodontol. 70 (1999) 151–158.
[50] J.A. Cottrell, F.M. Vales, D. Schachter, S. Wadsworth, R. Gundlapalli, R. Kapadia, J.P. O'Connor, Osteogenic activity of locally applied small molecule drugs in a rat femur defect model, J. Biomed. Biotechnol. 2010 (2010) 597641.
[51] H. Schell, J. Lienau, D.R. Epari, P. Seebeck, C. Exner, S. Muchow, H. Bragulla, N.P. Haas, G.N. Duda, Osteoclastic activity begins early and increases over the course of bone healing, Bone 38 (2006) 547–554.
[52] X.Z. Shu, K.J. Zhu, W. Song, Novel pH-sensitive citrate cross-linked chitosan film for drug controlled release, Int. J. Pharm. 212 (2001) 19–28.
[53] R. Pauliukaite, M.E. Ghica, O. Fatibello-Filho, C.M. Brett, Comparative study of different cross-linking agents for the immobilization of functionalized carbon nanotubes within a chitosan film supported on a graphite-epoxy composite electrode, Anal. Chem. 81 (2009) 5364–5372.
[54] V.L. Gonçalves, M. Laranjeira, V.T. Fávere, R.C. Pedrosa, Effect of crosslinking agents on chitosan microspheres in controlled release of diclofenac sodium, Polimeros 15 (2005) 6–12.
[55] M. Ishihara, M. Fujita, K. Obara, H. Hattori, S. Nakamura, M. Nambu, T. Kiyosawa, Y. Kanatani, B. Takase, M. Kikuchi, Controlled releases of FGF-2 and paclitaxel from chitosan hydrogels and their subsequent effects on wound repair, angiogenesis, and tumor growth, Curr. Drug Deliv. 3 (2006) 351–358.
[56] H.G. Bone, S. Adami, R. Rizzoli, M. Favus, P.D. Ross, A. Santora, S. Prahalada, A. Daifotis, J. Orloff, J. Yates, Weekly administration of alendronate: rationale and plan for clinical assessment, Clin. Ther. 22 (2000) 15–28.
[57] T. Van den Wyngaerta, M.T. Huizing, J.B. Vermorken, Osteonecrosis of the jaw related to the use of bisphosphonates, Curr. Opin. Oncol. 19 (2007) 315–322.
[58] S. Srisubut, A. Teerakapong, T. Vattraphodes, S. Taweechaisupapong, K. Kaen, Effect of local delivery of alendronate on bone formation in bioactive glass grafting in rats, Oral Surg. Oral Med. Oral Pathol. 104 (2007) E11–E16.
[59] C.W. Kim, Y.P. Yun, H.J. Lee, Y.S. Hwang, I.K. Kwon, S.C. Lee, In situ fabrication of alendronate-loaded calcium phosphate microspheres: controlled release for inhibition of osteoclastogenesis, J. Control. Release 147 (2010) 45–53.